

Dartmouth College

Dartmouth Digital Commons

Open Dartmouth: Published works by
Dartmouth faculty

Faculty Work

7-14-2005


Calmodulin and PF6 are components of a complex that localizes to the C1 microtubule of the flagellar central apparatus

Matthew J. Wargo
Dartmouth College

Erin E. Dymek
Dartmouth College

Elizabeth F. Smith
Dartmouth College

Follow this and additional works at: <https://digitalcommons.dartmouth.edu/facoa>

 Part of the [Biology Commons](#), and the [Cell Biology Commons](#)

Dartmouth Digital Commons Citation

Wargo, Matthew J.; Dymek, Erin E.; and Smith, Elizabeth F., "Calmodulin and PF6 are components of a complex that localizes to the C1 microtubule of the flagellar central apparatus" (2005). *Open Dartmouth: Published works by Dartmouth faculty*. 1740.
<https://digitalcommons.dartmouth.edu/facoa/1740>

This Article is brought to you for free and open access by the Faculty Work at Dartmouth Digital Commons. It has been accepted for inclusion in Open Dartmouth: Published works by Dartmouth faculty by an authorized administrator of Dartmouth Digital Commons. For more information, please contact dartmouthdigitalcommons@groups.dartmouth.edu.

Calmodulin and PF6 are components of a complex that localizes to the C1 microtubule of the flagellar central apparatus

Matthew J. Wargo, Erin E. Dymek and Elizabeth F. Smith*

Dartmouth College, Department of Biological Sciences, 301 Gilman Hall, Hanover, NH 03755, USA

*Author for correspondence (e-mail: elizabeth.f.smith@dartmouth.edu)

Accepted 14 July 2005

Journal of Cell Science 118, 4655–4665 Published by The Company of Biologists 2005
doi:10.1242/jcs.02585

Summary

Studies of flagellar motility in *Chlamydomonas* mutants lacking specific central apparatus components have supported the hypothesis that the inherent asymmetry of this structure provides important spatial cues for asymmetric regulation of dynein activity. These studies have also suggested that specific projections associated with the C1 and C2 central tubules make unique contributions to modulating motility; yet, we still do not know the identities of most polypeptides associated with the central tubules. To identify components of the C1a projection, we took an immunoprecipitation approach using antibodies generated against PF6. The *pf6* mutant lacks the C1a projection and possesses flagella that only twitch; calcium-induced modulation of dynein activity on specific doublet microtubules is also defective in *pf6* axonemes. Our antibodies specifically precipitated five polypeptides in addition to PF6. Using mass spectrometry, we determined

the amino acid identities of these five polypeptides. Most notably, the PF6-containing complex includes calmodulin. Using antibodies generated against each precipitated polypeptide, we confirmed that these polypeptides comprise a single complex with PF6, and we identified specific binding partners for each member of the complex. The finding of a calmodulin-containing complex as an asymmetrically assembled component of the central apparatus implicates the central apparatus in calcium modulation of flagellar waveform.

Supplementary material available online at
<http://jcs.biologists.org/cgi/content/full/118/20/4655/DC1>

Key words: Flagella, Axoneme, Calmodulin, Dynein, *Chlamydomonas*

Introduction

The complex waveforms characteristic of beating cilia and flagella result from spatial regulation of dynein activity along the axonemal microtubules. Numerous studies have indicated that the central apparatus plays a prominent role in spatially regulating dynein activity on specific subsets of doublet microtubules to modulate ciliary and flagellar waveform and possibly beat frequency (for a review, see Smith and Yang, 2004). Importantly, organisms with mutations that result in the failure of the entire central apparatus to assemble possess flagella that are paralyzed (Witman et al., 1978; Dutcher et al., 1984; Stannard et al., 2004). Flagellar motility can be restored in central pair-less *Chlamydomonas* strains by the introduction of a suppressor mutation (Huang et al., 1982), although the motility of these suppressed strains is not entirely wild-type (Brokaw et al., 1982). These suppressor mutations are typically in components of the dynein arms or the dynein regulatory complex (Huang et al., 1982; Piperno et al., 1992; Piperno et al., 1994; Porter et al., 1992; Porter et al., 1994). Axonemes isolated from central apparatus-defective mutants can be reactivated using low ATP concentrations to produce modest waveforms at very low beat frequency (Omoto et al., 1996). In similar studies using low concentrations of ATP, various salts and organic compounds, central pair-less axonemes were

reactivated with increased beat frequencies (~20 Hz) and larger amplitude waveforms (Yagi and Kamiya, 2000). Furthermore, isolated axonemes from central pair-less mutants reactivated at low ATP concentration also undergo modest waveform conversion in response to changes in calcium concentration (Wakabayashi et al., 1997; Frey et al., 1997). However, in all these cases motility of the central pair-less axonemes is not entirely the same as that of the wild type. Although the motility of the double mutant strains and reactivated central pair-less axonemes demonstrates that the central apparatus is not absolutely required for motility or waveform conversion, these studies imply a functional link between the central apparatus and dynein arm activity to produce wild-type motility.

The central apparatus is an asymmetric structure comprising two singlet microtubules, C1 and C2, that are structurally and biochemically distinct. Studies of *Chlamydomonas* mutants lacking specific central apparatus components have suggested that the inherent asymmetry of this structure provides important spatial cues for asymmetric regulation of dynein activity. For example, the *pf16* strain has flagella that are paralyzed or form rudimentary bends that do not propagate. Flagella of *pf16* mutants retain the C1 microtubule; yet, this central tubule is completely destabilized and solubilized upon demembration to produce axonemes (Dutcher et al., 1984; Smith and Lefebvre,

1996; Smith and Lefebvre, 2000). The flagella of the *cpc1* mutant lack the C1b projection and beat with a wild-type waveform, however, they beat at one-half the frequency of wild-type flagella (Mitchell and Sale, 1999; Zhang and Mitchell, 2004). The *pf6* mutant is defective in assembly of the C1a projection (Dutcher et al., 1984; Rupp et al., 2001); these flagella beat with a twitchy, uncoordinated waveform that is ineffective in propelling the cell through liquid media.

Our previous structural and functional studies of dynein-driven microtubule sliding provided evidence to indicate that calcium control of waveform includes modulation of the pattern of microtubule sliding between specific doublets (Wargo et al., 2004). This control mechanism is disrupted in certain mutants including the C1-defective mutant, *pf6* (Wargo et al., 2004). Our functional studies of dynein-driven microtubule sliding in isolated axonemes indicate that calmodulin and a calmodulin-dependent kinase may mediate the calcium signal and that the central apparatus and radial spokes are key components of the calcium signaling pathway (Smith, 2002b). Taken together, the motility phenotypes of C1-defective mutants combined with the results from our structural and functional studies suggest that the C1 central tubule is essential for wild-type motility and that each C1 projection makes a unique contribution to modulation of flagellar motility.

Understanding the role of the C1 microtubule in flagellar motility will require a complete molecular dissection of C1 components. To date, very few central apparatus polypeptides have been characterized (for a review, see Smith and Yang, 2004). Using two-dimensional gel electrophoresis to compare axonemes isolated from *Chlamydomonas* central apparatus-defective mutants, at least 23 polypeptides are associated with the central apparatus; 10 of these polypeptides are unique to the C1 microtubule, three of which are components of the C1a projection (Dutcher et al., 1984). Unfortunately, at the time these studies were completed, mass spectrometry and a complete *Chlamydomonas* genome sequence were not available to determine the identities of these polypeptides.

By taking advantage of an insertional mutagenesis approach, the amino acid sequences of several C1-associated polypeptides have now been determined. The wild-type *PF16* gene that encodes an armadillo repeat protein has been cloned (Smith and Lefebvre, 1996), as has the *CPC1* gene that encodes a protein with an adenylate kinase domain (Zhang and Mitchell, 2004). The predicted *PF6* gene product is a large (240 kDa), leucine-rich repeat protein that is predicted to form a scaffold for the assembly of additional polypeptides that comprise the C1a projection (Rupp et al., 2001). The PF6 protein sediments at 12S with at least four polypeptides that are not present in *pf6* axonemal extracts (Rupp et al., 2001). These results indicate that PF6 is extracted from the axoneme as a complex.

To specifically identify components of the C1a projection, we generated antibodies against PF6 and used these antibodies in immunoprecipitation experiments. The sequencing of the *Chlamydomonas reinhardtii* genome combined with advances in mass spectrometry provided the modern proteomics approaches necessary to identify the polypeptides comprising the C1 microtubule projections. Here, we report the identities of five polypeptides (in addition to PF6) that are specifically precipitated with anti-PF6 antibodies. Most notably, the PF6-containing complex includes calmodulin. In addition, we have

determined direct binding partners for these polypeptides. The finding of a calmodulin-containing complex as a component of the central apparatus further implicates the central apparatus in calcium modulation of flagellar waveform.

Materials and Methods

Strains and cell culture

Chlamydomonas reinhardtii strain A54-e18 (*nit1-1*, *ac17*, *sr1*, mt⁺) has wild-type motility and was obtained from Paul Lefebvre (University of Minnesota, St Paul, MN), the *cpc1-2* strain was from David Mitchell (SUNY, Syracuse, NY) and the *pf30pf28* strain from Winfield Sale (Emory University, Atlanta, GA). The strains *pf16*, *pf6-2*, *pf14* and *pf18* were obtained from the *Chlamydomonas* Genetics Center (Duke University). Cells were grown in constant light in TAP media (Gorman and Levine, 1965). *Chlamydomonas* strains cited in the text are listed in Table 1.

Axoneme isolation, protein extraction and sucrose gradient fractionation

Flagella were severed from cell bodies by the dibucaine method (Witman, 1986) and isolated by differential centrifugation in KLow (10 mM HEPES, pH 7.4, 5 mM MgSO₄, 1 mM DTT, 0.5 mM EDTA and 50 mM potassium acetate). Axonemes were isolated by adding NP-40 (Calbiochem, La Jolla, CA) to a final concentration of 0.5% (w/v). The axonemes were pelleted and resuspended in KLow. Protein concentration was determined using the Bradford assay (Bradford, 1976).

Axonemes were initially extracted in NaHigh (10 mM HEPES, pH 7.4, 5 mM MgSO₄, 1 mM DTT, 0.5 mM EDTA, 50 mM potassium acetate and 0.6 M NaCl) at a concentration of 6 mg/ml on ice for 20 minutes. The axonemes were pelleted, resuspended in NaHigh, and immediately pelleted again. The supernatant was discarded and the pellet was extracted with KI (10 mM HEPES, pH 7.4, 5 mM MgSO₄, 1 mM DTT, 0.5 mM EDTA, 50 mM potassium acetate and 0.5 M KI) at a concentration of 10–12 mg/ml for 20 minutes on ice. This extract is referred to as the KI extract or high-salt extract. KI extracts were dialyzed against NaLow buffer (the same composition as KLow except with 75 mM NaCl and no potassium acetate) and clarified by centrifugation at 12,000 g for 10 minutes. For some experiments the clarified extracts were loaded onto 5–20% sucrose gradients and subjected to ultracentrifugation at 35,000 rpm for 16 hours in an SW41Ti rotor. Fractions (0.5 ml) were collected from the bottom of the tube and prepared for SDS-PAGE.

Silver staining

For silver staining, gel plates were first rinsed in 50% nitric acid, washed thoroughly in deionized water and rinsed with 95% ethanol. After electrophoresis, gels were fixed in 50% methanol, 0.1% glacial

Table 1. *Chlamydomonas* strains used in this study

Strain	Structural or motility defect
A54-e18	No axonemal structural defect/wild-type motility*
<i>pf16</i>	Defective in C1 stability in isolated axonemes/flagella paralyzed [†]
<i>pf18</i>	Lacks central apparatus/rigid paralyzed flagella [‡]
<i>pf6-2</i>	Lacks central apparatus C1a projection/flagella twitch ^{†,§}
<i>cpc1-2</i>	Lacks central apparatus C1b projection/reduced beat frequency [¶]
<i>pf14</i>	Lacks radial spokes/paralyzed flagella**
<i>pf28pf30</i>	Lacks outer dynein arms and inner dynein arms I ^{††,‡‡}

*Smith and Lefebvre, 1996; [†]Dutcher et al., 1984; [‡]Witman et al., 1972; [§]Rupp et al., 2001; [¶]Mitchell and Sale, 1999; ^{**}Piperno et al., 1977; ^{††}Piperno et al., 1990; ^{‡‡}Smith and Sale, 1992.

acetic acid. Fixed gels were rinsed in deionized water for 8 minutes and then shaken in 0.001 mM DTT for 25 minutes. The DTT solution was replaced with a 0.1% aqueous silver nitrate solution. Following a 25 minute incubation in silver nitrate solution, the gel was rinsed quickly three times in deionized water and developed by the addition of 0.02% (v/v) formaldehyde in 3% sodium carbonate. Color development was halted by the addition of a one-quarter volume of 2 M citric acid.

Mass spectrometry, RNA isolation and RT-PCR

Gel bands were excised from Coomassie-stained gels. These bands were analyzed by MALDI-TOF (matrix-assisted laser desorption/ionization-time of flight) mass spectrometry with PSD (post-source decay) conducted at the University of Massachusetts Medical School (Worcester, MA) or LC/LC-ESI (liquid chromatography/liquid chromatography-electrospray ionization) mass spectrometry performed at Harvard Microchemistry and Proteomics Facility (Cambridge, MA). Comparisons of peptide masses with translated genomic or EST sequences were made using the Sequest algorithm (Eng et al., 1994) and the *Chlamydomonas* genome database (<http://genome.jgi-psf.org/chlre2/chlre2.home.html>). The complete coding sequence for each polypeptide was confirmed by RT-PCR.

RNA was isolated from wild-type *Chlamydomonas reinhardtii* cells after pH shock-induced deflagellation (Wilkerson et al., 1994). Poly(A) enrichment was performed using the Oligotex mRNA Kit according to the manufacturer's instructions (Qiagen, Valencia, CA). Reverse transcription was performed using either Superscript II or Superscript III according to the manufacturer's instructions (Invitrogen, Carlsbad, CA). Subsequent polymerase chain reactions were performed using primers based on the known or predicted coding regions as determined by EST, EST-contig or mass spectrometry data.

Construction of expression constructs, antibody production and affinity purification

Polyclonal antibodies for PF6, PF6-IP2, -IP3 and -IP4 were generated against bacterially expressed proteins in rabbits. For PF6, the genomic DNA template encoding amino acids 199-283 was amplified by PCR. For PF6-IP2, RT-PCR was used to generate a cDNA encoding amino acids 4-143. For PF6-IP3, RT-PCR was used to generate a cDNA encoding amino acids 2-267. For PF6-IP4, RT-PCR was used to generate a cDNA encoding amino acids 24-144. In all cases, the resulting PCR products were first ligated into the PCR2.1 vector using the TOPO-TA cloning kit (Invitrogen). The PCR fragments were then shuttled into the pET30 series of expression vectors (Novagen, Madison, WI). Proper orientation and reading frame were confirmed by DNA sequencing.

The above 6×His-tagged constructs were transformed into BL21 *E. coli* cells containing the pLysS plasmid (Novagen). Expression was induced by the addition of IPTG to a final concentration of 2 mM. For antibody production, proteins were isolated and purified using the manufacturer's denaturing protocol. Peak fractions were dialyzed against 4 M urea buffer (20 mM Tris-HCl, pH 7.9, 500 mM NaCl, 4 M urea) fixed with SDS sample buffer, and run on SDS-polyacrylamide gels. Protein bands were excised from Coomassie-stained gels and used for polyclonal antibody production in rabbits. Rabbits were injected with 100-200 µg of protein per injection, three times for a standard protocol (PF6, PF6-IP2 and PF6-IP3) or four times for an extended protocol (PF6-IP4). Handling of rabbits including all injections and bleeds was conducted by Spring Valley Laboratories (Woodbine, MD).

For affinity purification of antibodies PF6, PF6-IP2 and PF6-IP3 proteins were prepared from bacteria using the above protocol with guanidine-HCl in place of urea. These protein fractions were conjugated to Aminolink columns (Pierce Biotechnology, Rockford,

IL) according to the manufacturer's protocol and used for affinity purification. For affinity purification of PF6-IP4 antibodies, two cysteine residues were engineered at the C-terminus of the expressed PF6-IP4 protein. The protein resulting from this construct was purified using the urea protocol and conjugated to Sulfolink resin (Pierce) according to the manufacturer's instructions.

Peptide antibodies were generated against PF6-IP1 and calmodulin. For PF6-IP1 a peptide was synthesized corresponding to amino acids 791-808 (GRDEDEGGLLPVPEPWQC). For anti-calmodulin antibodies a peptide was synthesized representing the 17 C-terminal amino acids. This peptide (RMMTSGATDDKDKKGHK) is unique to *Chlamydomonas* calmodulin. For both the PF6-IP1 and calmodulin peptides, the peptides were conjugated to KLH and injected into rabbits for polyclonal antibody production. Peptide synthesis, peptide conjugation and antibody production was performed at Spring Valley Laboratories (Woodbine, MD). The resulting antibodies were affinity purified using the appropriate peptide conjugated to a Sulfolink column according to the manufacturer's instructions (Pierce).

Western blotting

For western blots, proteins were transferred from gels to PVDF membrane (Immobilon, Millipore, Billerica, MA). Blots were blocked with 5% non-fat dry milk in TBS-T (150 mM NaCl, 20 mM Tris-HCl pH 7.6, 0.1% Tween-20) and then incubated in primary antibody for 2 hours at room temperature. Affinity-purified antibodies were used at the following dilutions: anti-PF6, 1:1000; anti-PF6-IP1, 1:3000; anti-PF6-IP2, 1:500; anti-PF6-IP3, 1:2000; and anti-PF6-IP4, 1:100. Blots were incubated in secondary antibody (HRP-conjugated donkey anti-rabbit IgG (Amersham Biosciences Buckinghamshire, UK) diluted 1:30,000 for 45 minutes at room temperature in TBS-T. ECL+ solutions were used as directed by the manufacturer (Amersham Biosciences).

For western blots using anti-calmodulin antibodies, the proteins were transferred to PVDF, the membranes rinsed quickly in TBS (150 mM NaCl, 20 mM Tris-HCl pH 7.6), and then fixed in TBS with 0.2% glutaraldehyde for 30 minutes. The blot was rinsed for 5 minutes in TBS and blocked for 1 hour in TBS with 5% BSA (Sigma-Aldrich, St Louis, MO, regular fraction V, A-7906). After a brief rinse in TBS, blots were incubated with anti-calmodulin antibody (1:7000) in TBS with 1% BSA. After primary incubation, the blots were washed with TBS-T (TBS with 0.05% Tween-20) and incubated with anti-rabbit secondary antibody as above but in TBS-T with 1% BSA. Final washes were carried out with TBS-T and ECL+ solutions were used as directed.

Immunoprecipitation

For immunoprecipitations from extracts, the affinity-purified antibody (30-70 µg), sample (300-750 µg dialyzed extract or undialyzed extract where noted) and TBS-T₁₅₀ (150 mM NaCl, 20 mM Tris-HCl, pH 7.5) were added to ~70 µl protein-A beads (Invitrogen) in a total volume of 600 µl. The sample was mixed for 1.5 hours at 4°C. Samples were washed four times with 500 µl TBS-T₁₅₀ for 5 minutes each. Unless noted, samples were prepared for SDS-PAGE by addition of 100 µl of 3× SDS sample buffer.

For immunoprecipitation using sucrose gradient fractions, 50-80 µg antibody were used with 1200 µl pooled sucrose gradient fractions. Tween-20 was added to a final concentration of 0.05% (v/v). The sample was mixed for 5-8 hours and washed with four 1 ml volumes of TBS-T₁₅₀.

Blot overlay

PF6-IP3::6×His protein for blot overlays was isolated from bacteria as described above, except no urea was used. Axonemal proteins were blotted onto nitrocellulose and blocked in TBS-T with 5% milk

overnight at 4°C. The PF6-IP3::6×His protein was diluted to 4 µg/ml in TBS with 1% BSA and incubated with the blot for 2.5 hours at room temperature. Overlaid protein was detected using S-protein overlay with HRP-S-protein (Novagen) diluted 1:5000 in TBS-T. S-protein was visualized with ECL⁺ according to the manufacturer's instructions.

Results

Immunoprecipitation of a PF6-containing complex

Based on the *pf6* mutant phenotype, the C1a projection is evidently important for ciliary and flagellar motility. The PF6 protein is large and predicted to form a scaffold that is required for the assembly and/or stability of the C1a central pair projection (Rupp et al., 2001). To begin defining the polypeptides associated with the C1a projection, we generated antibodies against PF6 and used them in immunoprecipitation experiments. We expressed 289 amino acids at the C-terminus of PF6 in bacteria, and then used the purified expressed protein to generate polyclonal antibodies in rabbits (see Materials and Methods). These antibodies are specific and recognize a polypeptide of high molecular weight consistent with that of PF6 in wild-type axonemes that is absent from axonemes isolated from the *pf6* mutant (Fig. 1A).

PF6 sediments at approximately 12S on sucrose gradients indicating that it is extracted as a complex (Rupp et al., 2001). To identify the components of this complex we used our anti-PF6 antibodies to precipitate PF6 from dialyzed, axonemal salt extracts. As a negative control, we also used axonemal extracts isolated from the *pf6* mutant. Our anti-PF6 antibodies reproducibly precipitate five polypeptides in addition to PF6, which we tentatively named PF6-IP1 to PF6-IP5 (Fig. 1B). These polypeptides range in relative molecular mass from approximately 75 kDa to 20 kDa and are not precipitated from axonemal extracts isolated from the *pf6* mutant.

Identification of polypeptides comprising the PF6 complex using mass spectrometry

To determine the amino acid identities of the polypeptides precipitated by our anti-PF6 antibodies, the bands corresponding PF6-IP1, -IP2, -IP3 and -IP4 were excised from polyacrylamide gels and subjected to mass spectrometry; peptide masses were compared with those predicted from the translated *Chlamydomonas* genome and EST databases (see Materials and Methods). The results of these analyses are shown in Table 2.

The complete amino acid sequence for PF6-IP1 was determined from searches of the *Chlamydomonas* genomic database using 43 peptide masses. In addition, two ESTs were identified, one of which was in the 5'-UTR, the other in the 3'-UTR. The PF6-IP1 gene is predicted to encode an 835 amino

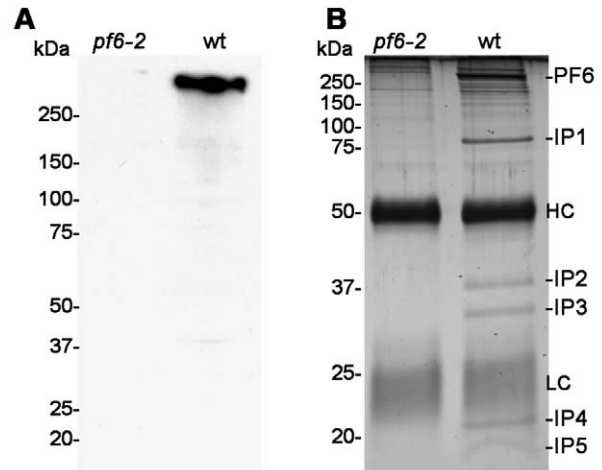


Fig. 1. (A,B) Western blots of axonemes and silver-stained gel of immunoprecipitates. (A) Western blot of axonemes isolated from wild-type (wt) and *pf6-2* *Chlamydomonas reinhardtii* cells probed with our anti-PF6 antibodies. A band with a molecular weight consistent with that of PF6 is present in wild-type axonemes and absent in *pf6-2* axonemes. (B) Silver-stained gel of immunoprecipitates obtained from wild-type (wt) and *pf6-2* axonemal extracts using our anti-PF6 antibodies. In wild-type axonemal extracts, five polypeptides in addition to PF6 are specifically precipitated using anti-PF6 antibodies. These polypeptides are not precipitated in *pf6-2* axonemal extracts. The precipitating immunoglobulin heavy and light chains are labeled HC and LC, respectively.

acid protein with a calculated isoelectric point of 5.54 (v2; scaffold 2: 712,757-717,357; GenBank accession DQ119666; based on proximity to the GSP1 marker, the PF6-IP1 gene is on LGII). In searches of translated databases, PF6-IP1 is most similar (29% identity, 51% similarity over 102 amino acids) to protein kinase A regulatory subunits within an RII-like leucine-rich repeat region. However, PF6-IP1 lacks canonical cAMP binding sites. The PF6-IP1 protein may correspond to the ~84 kDa protein that is reported to co-sediment with PF6 on sucrose gradients (Rupp et al., 2001).

The amino acid sequence of PF6-IP2 was determined from the *Chlamydomonas* genomic and EST databases using three peptide masses (Table 2; peptides: DLSSAQLESIR, RLQEEYEEAAIPEEVK, and VMDWMLDSYYR). The PF6-IP2 gene is predicted to encode a 306 amino acid protein with a calculated isoelectric point of 5.63 (v2; scaffold 20: 996,339-997,738; GenBank accession DQ119665; based on proximity to the TPX marker, the PF6-IP2 gene is on LGVI). PF6-IP2 is 48% similar, 30% identical to the mouse protein GM166 over a stretch of 207 amino acids. The PF6-IP2 protein has a small, predicted coiled-coil region from amino acids 172 to 219, but contains no other predicted structural motifs. This

Table 2. Summary of mass spectrometry data and similarity searches

IP band	kDa	Peptides	BLAST results (most similar to)	Cilia proteome*	Proposed name
PF6-IP1	86	45	<i>T. brucei</i> PKA regulatory subunit ($E=4e-04$)	FAP 101	C1a-86
PF6-IP2	34	3	Unnamed <i>T. nigroviridis</i> protein ($E=4e-14$)	FAP119	C1a-34
PF6-IP3	32	1	Gm166 protein from <i>M. muscalis</i> ($E=2e-06$)	FAP114	C1a-32
PF6-IP4	18	1	<i>T. brucei</i> hypothetical protein ($E=2e-27$)	FAP227	C1a-18

*Pazour et al. (2005).

protein may be identical to the ~43 kDa protein reported to co-sediment with PF6 on sucrose gradients (Rupp et al., 2001).

The amino acid sequence of the PF6-IP3 protein was determined from the *Chlamydomonas* genomic and EST databases using one peptide mass (Table 2; peptide: KPATLEEAIHLVATR). Numerous overlapping ESTs comprised the complete coding sequence for PF6-IP3 (Contig 20021010.4549.3). The PF6-IP3 gene encodes a predicted 286 amino acid protein with a calculated isoelectric point of 5.56 (v2; scaffold 8: 1,039,925-1,043,440; GenBank accession DQ119664; telomeric to YPTC4 on LGII). Like PF6-IP2, PF6-IP3 is similar to the Gm166 protein from mouse brain with 47% similarity, 26% identity over a stretch of 129 amino acids. In addition, proteins with weak similarity are found in *Rattus norvegicus*, *Tetraodon nigroviridis*, *Canis familiaris* and *Gallus gallus* databases. Although there are no obvious functional domains in PF6-IP3, the protein contains two predicted coiled-coil regions that are well supported by the Coils (Lupas et al., 1991) and the Paircoil (Berger et al., 1995) algorithms. Interestingly, when sequence comparisons are conducted using the pair-wise blastp algorithm (Tatusova and Madden, 1999), the 150 N-terminal amino acids of PF6-IP2 and PF6-IP3 align with 22% identity and 41% similarity (supplementary material Fig. S1). If the alignment is conducted without the low complexity filter, these two proteins align with 26% identity and 42% similarity along their entire length. This slight difference is due to the significant number of alanine residues in the carboxyl half of both proteins.

The amino acid sequence of the PF6-IP4 protein was determined from the *Chlamydomonas* genomic database using one peptide mass (Table 2; peptide: KFYYPGAIYEGQWK). Predicted intron and exon boundaries were confirmed by RT-PCR (see Materials and Methods). The PF6-IP4 cDNA encodes a predicted 173 amino acid protein with a calculated isoelectric point of 5.70 (v2; scaffold 1:101,203-103,216; coding sequence GenBank accession DQ119663; centromeric to the S926 marker from LGXIX) (Kathir et al., 2003). Searches of translated databases reveal similar proteins in the flagellated organisms *Leishmania major*, *Trypanosoma brucei* and *Cyprinus carpio*. All these proteins contain MORN (membrane occupation and recognition nexus) domains, with similarity to MORN domain-containing phosphatidylinositol 4-phosphate-5-kinases in vascular plants. Based on molecular mass, predicted isoelectric point and its absence in *pf6* axonemes, the PF6-IP4 protein may correspond to CP18 described previously (Dutcher et al., 1984).

PF6-IP5 is calmodulin

Axonemal calmodulin is extractable and sediments in three distinct peaks of approximately 21S, 12S and 6S on sucrose gradients (Yang et al., 2001). The 21S peak corresponds to calmodulin associated with the radial spokes. The 12S peak of calmodulin is thought to be associated with the central apparatus (P. Yang, Marquette University, Milwaukee, WI, personal communication). We generated anti-calmodulin antibodies that recognize the unique C-terminus of *Chlamydomonas* calmodulin and that are of higher affinity than commercially available anti-calmodulin antibodies (see Materials and Methods). Using our anti-calmodulin antibodies

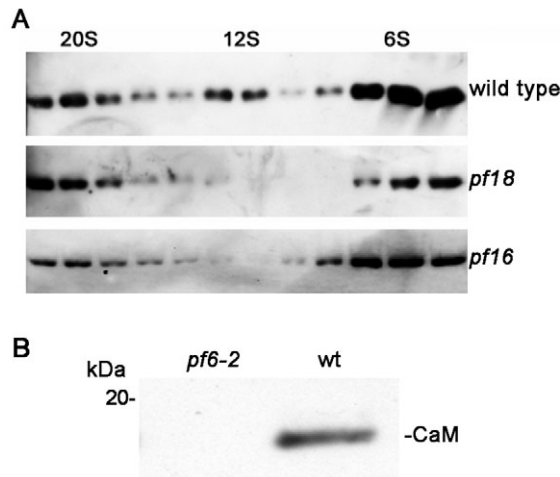


Fig. 2. (A,B) Western blots of sucrose gradient fractions and immunoprecipitates. (A) Western blots of axonemal extracts obtained from wild-type, *pf18* and *pf16* axonemes fractionated on 5-20% sucrose gradients. Blots were probed with our anti-calmodulin antibodies. Calmodulin sediments in three distinct peaks. The 12S peak of calmodulin is lacking or severely reduced in central pair-defective mutants. (B) Western blots of immunoprecipitates obtained from wild-type (wt) and *pf6-2* axonemal extracts using our anti-PF6 antibodies. The blot was probed with anti-calmodulin antibodies. Calmodulin is precipitated by anti-PF6 antibodies from wild-type extracts.

we probed sucrose gradient fractions of axonemal extracts prepared from the wild type and central apparatus-defective mutants. The 12S peak of calmodulin was not present or extremely reduced in extracts isolated from *pf18* and *pf16* (Fig. 2A) suggesting the calmodulin is associated with the C1 microtubule of the central apparatus. Based on this observation and the apparent molecular weight of PF6-IP5 we suspected that this polypeptide was calmodulin. Western blots of our PF6 immunoprecipitates probed with our anti-calmodulin antibodies confirmed that PF6-IP5 is in fact calmodulin (Fig. 2B).

PF6-IP1, IP2, IP3, IP4 and calmodulin are components of a single PF6-containing complex that localizes to the C1a projection

To confirm that the proteins we precipitated correspond to a PF6-containing complex that localizes to the C1a projection, we bacterially expressed PF6-IP1, -IP2, -IP3 and -IP4 and used the purified proteins for polyclonal antibody production in rabbits. Each of these antibodies is specific and recognizes a protein of the correct molecular weight on blots of wild-type axonemes (Fig. 3A,B). The failure of PF6-IP1, -IP2, -IP3 and -IP4 to assemble in *pf6* mutant axonemes strongly suggests their localization to the C1a projection.

Western blots using our anti-PF6, PF6-IP1, -IP2, -IP3, -IP4 and calmodulin antibodies revealed that each of these polypeptides is precipitated using our anti-PF6 antibodies (Fig. 4). To determine if PF6 is present in multiple complexes containing subsets of these five polypeptides or if the PF6 immunoprecipitate represents one large complex, we then used antibodies generated against PF6-IP1, -IP2, -IP3, -IP4 and

microtubule is solubilized. Our anti-PF6 antibodies precipitated all members of the PF6-containing complex from the *pfl6* membrane-matrix fraction (data not shown). These experiments provide additional confirmation that we have identified all members of the PF6 complex and that their interactions are not dependent on high-salt extraction and subsequent dialysis.

PF6 sediments at approximately 12S on sucrose gradients

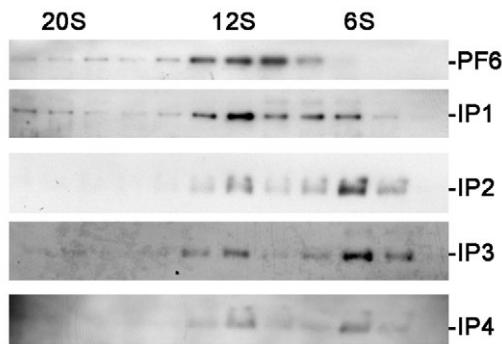


Fig. 5. Western blots of axonemal extracts obtained from wild-type axonemes fractionated on 5-20% sucrose gradients. Blots were probed with antibodies generated against the proteins noted to the right of each panel. PF6 and PF6-IP1, -IP2, -IP3 and -IP4 sediment in two peaks.

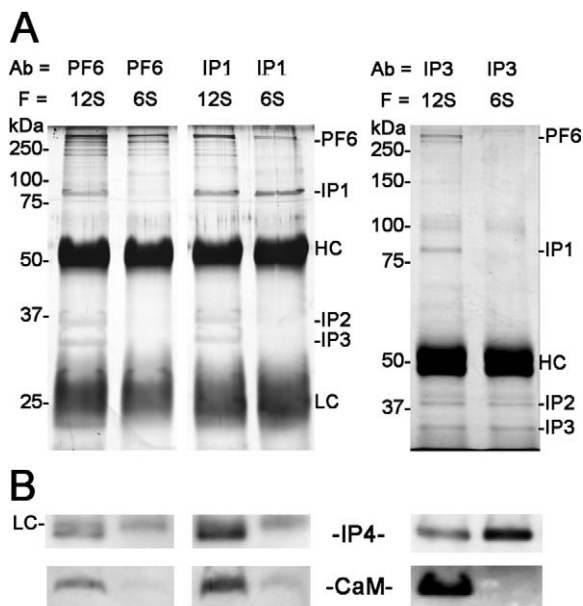


Fig. 6. (A,B) Silver-stained gels and corresponding western blots of immunoprecipitates. (A) Silver-stained gels of immunoprecipitation experiments performed from pooled sucrose gradient fractions. The precipitating antibodies (Ab) and the fractions (F) used for each experiment are noted at the top of the lanes. The panel on the left is an 8% polyacrylamide gel whereas the panel on the right is a 12% polyacrylamide gel. The precipitating immunoglobulin heavy and light chains are labeled HC and LC, respectively. (B) Corresponding western blots using our anti-calmodulin and anti-PF6-IP4 antibodies. All six polypeptides in the PF6 complex precipitate from the 12S fraction. Only subsets of these polypeptides are precipitated from the 6S fraction.

(Rupp et al., 2001) and as indicated in Fig. 2, calmodulin also sediments at 12S. Therefore, we predicted that PF6-IP1, -IP2, -IP3 and -IP4 would co-sediment at 12S. Western blots of dialyzed wild-type axonemal extracts fractionated on sucrose gradients revealed that these four polypeptides sediment in two peaks, 12S and approximately 6S (Fig. 5). We suspected that the 6S peak represented either subunits of the larger 12S peak that had dissociated, or subunits of the 12S complex that failed to re-associate during dialysis of the high-salt extract. Distinguishing between these possibilities provided an opportunity to begin determining precise binding partners for each of the complex components.

Direct interactions between components of the PF6 complex

To determine the composition of the 12S and 6S sedimenting complexes, we performed immunoprecipitation experiments from corresponding sucrose gradient fractions using our anti-PF6 antibodies. The anti-PF6 antibodies precipitate PF6, PF6-IP1, -IP2, -IP3 and -IP4 and calmodulin from the 12S fraction, however, only PF6 is precipitated from the 6S fraction (Fig. 6A,B, left panel). We also performed immunoprecipitation experiments from the 12S and 6S fractions using our anti-PF6-IP1 and anti-PF6-IP3 antibodies. The anti-PF6-IP1 antibodies precipitate PF6, PF6-IP1, -IP2, -IP3 and -IP4 as well as calmodulin from the 12S fraction; however, only PF6-IP1 and small amounts of PF6 and calmodulin were precipitated from the 6S fraction. Using our anti-PF6-IP3 antibodies PF6, PF6-IP1, -IP2, -IP3 and -IP4 were immunoprecipitated from the 12S fractions (Fig. 6A,B, right panel). However, in experiments using the 6S fractions, only PF6-IP2, -IP3 and -IP4 were detected in the anti-PF6-IP3 immunoprecipitates (Fig. 6A,B, right panel); there is no detectable PF6, PF6-IP1, or calmodulin precipitated from this fraction. These results provide further confirmation that these five components form a single complex that includes PF6 and calmodulin and suggest that PF6-IP2, -IP3 and -IP4 interact with each other.

To determine if dialysis is required to form the 12S complex and further define binding partners for specific polypeptides, we conducted immunoprecipitation experiments from undialyzed, high-salt extracts (Fig. 7). Under high-salt conditions, our anti-PF6 antibodies precipitate PF6 and minimal amounts of PF6-IP2, -IP3 and calmodulin. Both our anti-PF6-IP1 and anti-calmodulin antibodies precipitate both PF6-IP1 and calmodulin, suggesting that PF6-IP1 and calmodulin directly interact. Our anti-PF6-IP3 antibodies precipitate PF6-IP2, PF6-IP3 and PF6-IP4 and very minimal amounts of PF6. These studies provide additional evidence that PF6-IP2, -IP3 and -IP4 directly interact and suggest that the 12S complex reforms during dialysis.

Based on our precipitation results using undialyzed high-salt extracts, we suspected that the 12S complex only partially reforms upon dialysis resulting in complexes that sediment at 6S as well as 12S. To test this hypothesis, we fractionated non-dialyzed axonemal extracts on high-salt sucrose gradients. PF6, PF6-IP1, -IP2, -IP3, -IP4 and calmodulin all sediment at 6S with no detectable 12S peak (Fig. 8). These results support the hypothesis that the 12S PF6-containing complex requires dialysis to reassemble.

Our immunoprecipitation experiments suggest that PF6-IP3

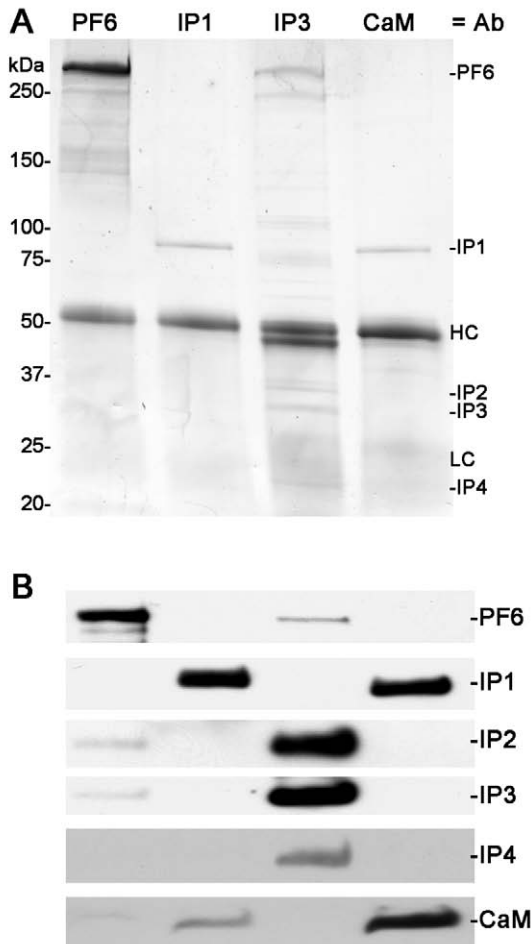


Fig. 7. (A,B) Silver-stained gels and corresponding western blots of immunoprecipitates. (A) Silver-stained gel of immunoprecipitation experiments using undialyzed, high-salt axonemal extracts obtained from wild-type flagella. The precipitating antibody is indicated at the top of each lane. The immunoglobulin heavy and light chains are labeled HC and LC, respectively. (B) Corresponding western blots from immunoprecipitation experiments. The blots were probed with the antibodies indicated to the right of each panel. In high-salt conditions, PF6-IP1 and calmodulin co-precipitate, and PF6-IP2, -IP3 and -IP4 co-precipitate. Only very minimal amounts of complex components precipitate with PF6.

interacts with PF6-IP2 and PF6-IP4. To determine whether PF6-IP3 directly interacts with PF6-IP2 or PF6-IP4 we used a blot overlay approach. Soluble, bacterially expressed PF6-IP3::6×His protein was used to probe a nitrocellulose blot of axonemal protein samples from a variety of strains. PF6-IP3 specifically interacted with a band of ~37 kDa that was absent from *pf6* axonemes and greatly reduced in *pf16* and *pf18* axonemes (Fig. 9). The molecular weight of this polypeptide and its absence in *pf6* axonemes strongly suggests that it is PF6-IP2.

Discussion

Phenotypic analyses of C1-defective mutants (e.g., Dutcher et al., 1984; Mitchell and Sale, 1999) as well as recent structural and functional studies (Smith, 2002a; Smith, 2002b; Wargo and Smith, 2003; Wargo et al., 2004) have provided ample

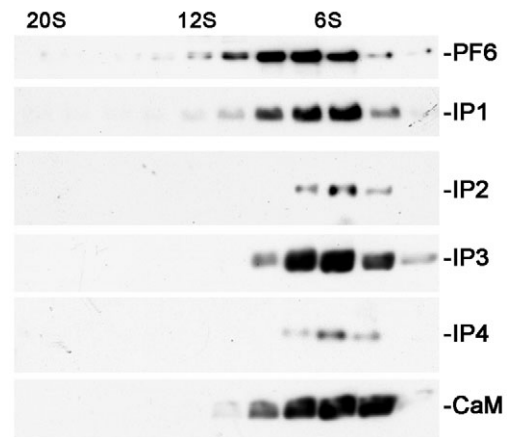


Fig. 8. Western blots of undialyzed high-salt axonemal extracts obtained from wild-type axonemes fractionated on 5-20% sucrose gradients. Blots were probed with antibodies generated against the proteins noted to the right of each panel. Under high-salt conditions, all six members of the PF6 complex sediment at 6S.

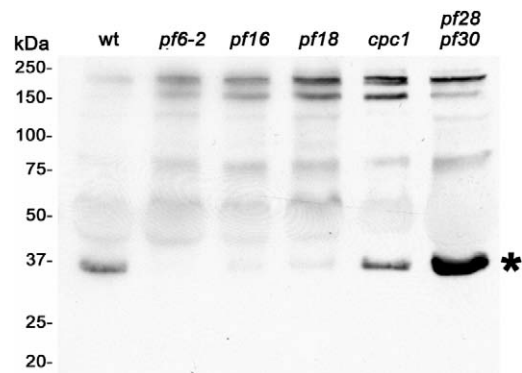


Fig. 9. Western blot of gel overlay assay. Axonemes from wild-type (wt) and mutant axonemes were subjected to SDS-PAGE and transferred to nitrocellulose membrane. The blot was then incubated with bacterially expressed PF6-IP3. The bound PF6-IP3 was detected using S-protein overlay (see Materials and Methods). PF6-IP3 binds to a polypeptide of molecular weight consistent with that of PF6-IP2 (asterisk). This polypeptide is absent in axonemes isolated from *pf6*, *pf16* and *pf18*, also consistent with PF6-IP2.

evidence to indicate that the C1 microtubule plays a role in regulation of motility. In addition, each C1 projection appears to make a unique contribution to modulation of flagellar motility. For example, we have shown that modulation of dynein activity on specific subsets of doublet microtubules in response to changes in calcium concentration is defective in *pf6* axonemes (Wargo et al., 2004). It is not yet clear whether this regulation involves structural or biochemical modification of axonemal components; these two possibilities are not mutually exclusive. In either event, understanding the molecular mechanism of this regulation will require identification of the polypeptides that comprise the C1 projections. We have taken an immunoprecipitation approach to begin defining the polypeptides comprising the C1a projection by using antibodies generated against a polypeptide (PF6) required for assembly of the C1a projection. We have

identified five polypeptides that form a complex with PF6, one of which is calmodulin, and have determined direct binding partners for these polypeptides.

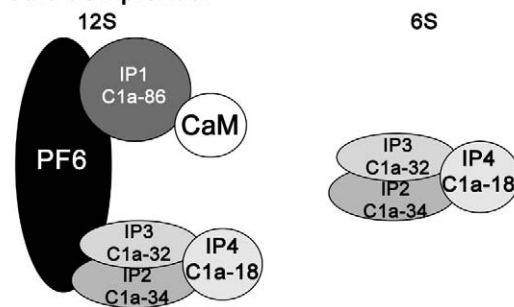
We tentatively named the four polypeptides (not including PF6 or calmodulin) that precipitated with our anti-PF6 antibodies, PF6-IP1, PF6-IP2, PF6-IP3 and PF6-IP4. All of these polypeptides have been identified in the recently reported *Chlamydomonas* flagellar proteome (see Table 2) (Pazour et al., 2005). Our conclusions that these polypeptides form a single complex with PF6 and calmodulin and localize to the C1a projection are based on the following results. First, all six polypeptides precipitate with our anti-PF6, anti-PF6-IP1, anti-PF6-IP3 and anti-calmodulin antibodies. Although our anti-calmodulin antibodies precipitate additional polypeptides, precipitation experiments using mutant axonemes indicate that these polypeptides localize to other axonemal structures. Second, all six polypeptides cosediment at 12S on sucrose gradients. A subset of components sediments at 6S; however, precipitation experiments of undialyzed KI axonemal extracts indicate that this 6S fraction probably represents complexes that were disrupted during high-salt extraction and not reformed during dialysis. This conclusion is also supported by data from immunoprecipitation experiments using either undialyzed NaCl extracts from wild-type axonemes or detergent solubilized C1 components isolated from *pf16* axonemes. Finally, with the exception of calmodulin, all of these polypeptides are lacking from *pf6* mutant axonemes. As noted above, calmodulin is present in other structures in the axoneme including the radial spokes (Yang et al., 2001). Based on these combined results, we propose to give PF6-IP1, -IP2, -IP3 and -IP4 the following names, C1a-86, C1a-34, C1a-32 and C1a-18, based on their calculated molecular weight and apparent localization within the axoneme (Table 2). We have obtained no data to support the hypothesis that PF6 interacts with either PF16 or PF20 (see Zhang et al., 2002; Zhang et al., 2005).

Although none of these polypeptides appear to be the *Chlamydomonas* homologues of proteins with known function, PF6-IP1, -IP3 and -IP4 contain previously characterized protein-protein interaction motifs. The PF6-IP1 protein contains leucine-rich repeats that are most similar to those from PKA regulatory proteins. PF6-IP3 has two predicted coiled-coil domains, and PF6-IP4 has three MORN domains.

The lack of an intact regulatory RII dimerization domain does not preclude a role for PF6-IP1 as a PKA regulatory subunit, as PKAs of both *Paramecium* and *Dictyostelium* have subunits that do not have RII domains (Mutzel et al., 1987; Carlson and Nelson, 1996). In addition, the leucine-rich repeat region of PF6-IP1 aligns with the CAP_ED domain of the *Trypanosoma* predicted regulatory subunit (29% identity, 51% similarity). The CAP_ED domain (CD00038) (Marchler-Bauer et al., 2005) is a conserved set of amino acids that binds cyclic nucleotides or assists in the binding of flavin groups; the predicted trypanosome CAP_ED-containing protein has been shown to stimulate the PKA catalytic subunit in a cAMP-dependent manner (Seebeck et al., 2001). The similarity of PF6-IP1 and the trypanosome CAP_ED suggests that PF6-IP1 may function as an unconventional regulatory subunit.

The MORN domains found in PF6-IP4 were first described to be required for plasma membrane binding in human

Low Salt Complexes:



High Salt Complexes:

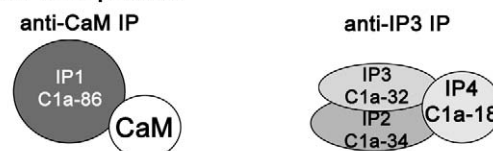


Fig. 10. Models of C1a components and their interactions based on the immunoprecipitation and sucrose gradient data in both high-salt and low-salt conditions.

junctophilins (Takeshima et al., 2000). Recently, the amino acid sequences of two polypeptides associated with the radial spoke head were determined and found to have repeated MORN motifs (P. Yang, personal communication). The presence of multiple MORN motif-containing polypeptides in the axonemes suggests their importance in assembly and/or function of the organelle. One hypothesis is that the MORN motifs function like the junctophilin MORN motifs and allow association with the flagellar membrane. This association may be required for correct assembly of axonemal components by intraflagellar transport. Alternatively, the MORN motif may represent a novel folding motif used to generate a characteristic structure and used for a variety of functions.

We have also begun to determine interactions between individual components of the complex. A summary diagram illustrating these complexes and their interactors is shown in Fig. 10. Based on sucrose gradient sedimentation and immunoprecipitation using undialyzed KI high-salt extracts, PF6-IP1 interacts with calmodulin. PF6-IP2, PF6-IP3 and PF6-IP4 appear to form a sub-complex in which PF6-IP3 directly interacts with PF6-IP4. Both the PF6-IP1/calmodulin and the PF6-IP2/-IP3/-IP4 sub-complexes are stable in high salt concentrations. However, the 12S complex contains all six polypeptides requires dialysis into low salt concentrations to reform. Although it is possible that dialysis induces formation of a large complex that does not naturally occur in the axoneme, we think this possibility is unlikely. All six polypeptides precipitate from undialyzed NaCl extracts isolated from wild-type axonemes, all six polypeptides precipitate from the membrane matrix fraction isolated from *pf16* axonemes, and all six polypeptides are absent from *pf6* mutant axonemes, indicating that PF6 is required for their assembly.

Important questions we have yet to consider are: have we identified all of the polypeptides that correspond to the C1a

projection and what is the relative stoichiometry of the constituent polypeptides of this complex? The C1a projection is approximately 20 nm in length and 4 nm in width. The PF6 protein has a molecular weight of 237 kDa. Based on the assumption that the partial specific volume for soluble, globular proteins is approximately 0.73 cm³/g, PF6 would occupy a volume of 287 nm³. If we assume that PF6 is present in a more extended rectangular form, this volume could be occupied by a rectangular block 4 nm in both length and width and 18 nm in height. These dimensions are not significantly different from that of the C1a projection. When the volumes of the polypeptides we identified as components of the PF6 complex are considered, it seems reasonable to conclude that these polypeptides may form the C1a projection in its entirety. We have performed two-dimensional gel electrophoresis of our precipitated proteins to rule out the possibility that additional components are obscured by the antibody heavy and light chains (not shown). As far as we can ascertain given that our antibodies are polyclonal, we have identified all of the members of the precipitated complex. However, we cannot rule out the possibility that there may be additional minor components that are dissociated and are not precipitated by the PF6 antibodies.

We have attempted microtubule binding experiments using both axonemal extracts and 12S sucrose gradient fractions to investigate whether this complex can bind to microtubules assembled from purified tubulin *in vitro*. So far, this complex has failed to sediment with microtubules. These results may indicate that an as yet unidentified adaptor complex is required for binding these C1a projection components to microtubules. Alternatively, it is possible that this complex must assemble concurrently with microtubule assembly. However, as dikaryon rescue experiments with *pf6* mutants are successful (Dutcher et al., 1984), this possibility seems unlikely.

Another important question to answer is, what are the precise functions of the individual polypeptides we identified? With the exception of *pf6*, the genes encoding the members of this complex do not map to previously identified mutations. To determine if any one polypeptide plays a role in regulating motility we are pursuing RNAi knockdown of transcript levels. We predict that the mutant motility phenotype will not be as severe as that of *pf6* but not wild-type. So far, our attempts at reducing expression levels of PF6-IP2 and -IP3 have been unsuccessful. We are currently generating constructs for PF6-IP1 and -IP4 for RNAi silencing.

Our previous studies have suggested a possible role for the C1a projection in calcium regulation of flagellar motility (Smith, 2002b; Wargo et al., 2004). The finding that calmodulin, an important calcium sensor, is a component of the C1a complex is an exciting result and further implicates this structure in calcium modulation of motility. This complex may regulate the detection and/or transmission of a calcium regulatory signal to the radial spokes. As calmodulin plays many important roles in cell function, it is not feasible to knock down calmodulin expression to ascertain its role in flagellar motility. However, based on our finding that the central apparatus calmodulin binds to PF6-IP1, knockdown of PF6-IP1 may provide clues as to the role of central apparatus associated calmodulin in calcium detection and waveform modulation.

The authors gratefully acknowledge the help of Heather Benson (Dartmouth College) in the preparation of PF6-IP1 for mass spectrometry and Pinfen Yang (Marquette University) for sharing unpublished results. This work was supported by NIH grant GM66919 (E.F.S.) and NIH training grant GM08704-06 (M.J.W.).

References

- Berger, B., Wilson, D. B., Wolf, E., Tonchev, T., Milla, M. and Kim, P. S.** (1995). Predicting coiled coils by use of pairwise residue correlations. *Proc. Nat. Acad. Sci. USA* **92**, 8259-8263.
- Bradford, M. M.** (1976). A rapid and sensitive method for the quantitation of microgram quantities of protein utilizing the principle of protein-dye binding. *Anal. Biochem.* **72**, 248-254.
- Brokaw, C. J., Luck, D. J. and Huang, B.** (1982). Analysis of the movement of *Chlamydomonas* flagella: the function of the radial-spoke system is revealed by comparison of wild-type and mutant flagella. *J. Cell Biol.* **92**, 722-732.
- Carlson, G. L. and Nelson, D. L.** (1996). The 44-kDa regulatory subunit of the *Paramecium* cAMP-dependent protein kinase lacks a dimerization domain and may have a unique autophosphorylation site sequence. *J. Euk. Microbiol.* **43**, 347-356.
- Dutcher, S. K., Huang, B. and Luck, D. L.** (1984). Genetic dissection of the central pair microtubules of the flagella of *Chlamydomonas reinhardtii*. *J. Cell Biol.* **98**, 229-236.
- Eng, J. K., McCormack, A. L. and Yates, J. R., III** (1994). An approach to correlate tandem mass spectral data of peptides with amino acid sequences in a protein database. *J. Am. Soc. Mass Spectrom.* **5**, 9789.
- Frey, E., Brokaw, C. J. and Omoto, C. K.** (1997). Reactivation at low ATP distinguishes among classes of paralyzed flagella mutants. *Cell Motil. Cytoskeleton* **38**, 91-99.
- Gorman, D. S. and Levine, R. P.** (1965). Cytochrome f and plastocyanin: their sequence in the photosynthetic electron transport chain of *Chlamydomonas reinhardtii*. *Proc. Nat. Acad. Sci. USA* **54**, 1665-1669.
- Huang, B., Ramanis, Z. and Luck, D. J.** (1982). Suppressor mutations in *Chlamydomonas* reveal a regulatory mechanism for flagellar function. *Cell* **28**, 115-124.
- Kathir, P., LaVoie, M., Brazelton, W. J., Hass, N. A., Lefebvre, P. A. and Silflow, C. D.** (2003). Molecular map of the *Chlamydomonas reinhardtii* nuclear genome. *Eukaryot. Cell* **2**, 362-379.
- Lupas, A., Van Dyke, M. and Stock, J.** (1991). Predicting coiled coils from protein sequences. *Science* **252**, 1162-1164.
- Marchler-Bauer, A., Anderson, J. B., Cherukuri, P. F., DeWeese-Scott, C., Geer, L. Y., Gwadz, M., He, S., Hurwitz, D. I., Jackson, J. D., Ke, Z. et al.** (2005). CDD: a conserved domain database for protein classification. *Nucleic Acids Res.* **33**, D192-D196.
- Mitchell, D. R. and Sale, W. S.** (1999). Characterization of a *Chlamydomonas* insertional mutant that disrupts flagellar central pair microtubule-associated structures. *J. Cell Biol.* **144**, 293-304.
- Mutzel, R., Lacombe, M. L., Simon, M. N., de, Gunzburg, J. and Veron, M.** (1987). Cloning and cDNA sequence of the regulatory subunit of cAMP-dependent protein kinase from *Dictyostelium discoideum*. *Proc. Nat. Acad. Sci. USA* **84**, 6-10.
- Omoto, C. K., Yagi, T., Kurimoto, E. and Kamiya, R.** (1996). Ability of paralyzed flagella mutants of *Chlamydomonas* to move. *Cell Motil. Cytoskeleton* **33**, 88-94.
- Pazour, G. J., Agrin, N., Leszyk, J. and Witman, G. B.** (2005). Proteomic analysis of a eukaryotic cilium. *J. Cell Biol.* **170**, 103-113.
- Piperno, G., Mead, K. and Shestak, W.** (1992). The inner dynein arms I2 interact with a "dynein regulatory complex" in *Chlamydomonas* flagella. *J. Cell Biol.* **118**, 1455-1463.
- Piperno, G., Mead, K., LeDizet, M. and Moscatelli, A.** (1994). Mutations in the "dynein regulatory complex" alter the ATP-insensitive binding sites for inner arm dyneins in *Chlamydomonas* axonemes. *J. Cell Biol.* **125**, 1109-1117.
- Porter, M. E., Power, J. and Dutcher, S. K.** (1992). Extragenic suppressors of paralyzed flagellar mutations in *Chlamydomonas reinhardtii* identify loci that alter the inner dynein arms. *J. Cell Biol.* **118**, 1145-1162.
- Porter, M. E., Knott, J. A., Gardner, L. C., Mitchell, D. R. and Dutcher, S. K.** (1994). Mutations in the SUP-PF-1 locus of *Chlamydomonas reinhardtii* identify a regulatory domain in the beta-dynein heavy chain. *J. Cell Biol.* **126**, 1495-1507.

- Rupp, G., O'Toole, E. and Porter, M. E.** (2001). The *Chlamydomonas* PF6 locus encodes a large alanine/proline-rich polypeptide that is required for assembly of a central pair projection and regulates flagellar motility. *Mol. Biol. Cell.* **12**, 739-751.
- Seebeck, T., Gong, K. W., Kunz, S., Schaub, R., Shalaby, T. and Zoraghi, R.** (2001). cAMP signaling in *Trypanosoma brucei*. *Int. J. Parasit.* **31**, 491-498.
- Smith, E. F.** (2002a). Regulation of flagellar dynein by the axonemal central apparatus. *Cell Motil. Cytoskeleton* **52**, 33-42.
- Smith, E. F.** (2002b). Regulation of flagellar dynein by calcium and a role for an axonemal calmodulin and calmodulin-dependent kinase. *Mol. Biol. Cell* **13**, 3303-3313.
- Smith, E. F. and Lefebvre, P. A.** (1996). PF16 encodes a protein with armadillo repeats and localizes to a single microtubule of the central apparatus in *Chlamydomonas* flagella. *J. Cell Biol.* **132**, 359-370.
- Smith, E. F. and Lefebvre, P. A.** (2000). Defining functional domains within PF16: a central apparatus component required for flagellar Motility. *Cell Motil. Cytoskeleton* **46**, 157-165.
- Smith, E. F. and Yang, P.** (2004). The radial spokes and central apparatus: mechano-chemical transducers that regulate flagellar Motility. *Cell Motil. Cytoskeleton* **57**, 8-17.
- Stannard, W., Rutman, A., Wallace, C. and O'Callaghan, C.** (2004). Central microtubular agenesis causing primary ciliary dyskinesia. *Am. J. Respir. Crit. Care Med.* **169**, 634-637.
- Takeshima, H., Komazaki, S., Nishi, M., Iino, M. and Kangawa, K.** (2000). Junctophilins: a novel family of junctional membrane complex proteins. *Mol. Cell.* **6**, 11-22.
- Tatusuva, T. A. and Madden, T. L.** (1999). BLAST 2 Sequences, a new tool for comparing protein and nucleotide sequences. *FEMS Microbiol. Lett.* **174**, 247-250.
- Wakabayashi, K., Yagi, T. and Kamiya, R.** (1997). Ca²⁺-dependent waveform conversion in the flagellar axoneme of *Chlamydomonas* mutants lacking the central-pair/radial spoke system. *Cell Motil. Cytoskeleton* **38**, 22-28.
- Wargo, M. J. and Smith, E. F.** (2003). Asymmetry of the central apparatus defines the location of active microtubule sliding in *Chlamydomonas* flagella. *Proc. Nat. Acad. Sci. USA* **100**, 137-142.
- Wargo, M. J., McPeck, M. A. and Smith, E. F.** (2004). Analysis of microtubule sliding patterns in *Chlamydomonas* flagellar axonemes reveals dynein activity on specific doublet microtubules. *J. Cell Sci.* **117**, 2533-2544.
- Wilkerson, C. G., King, S. M. and Witman, G. B.** (1994). Molecular analysis of the gamma heavy chain of *Chlamydomonas* flagellar outer-arm dynein. *J. Cell Sci.* **107**, 497-506.
- Witman, G. B.** (1986). Isolation of *Chlamydomonas* flagella and flagellar axonemes. *Methods Enzymol.* **134**, 280-290.
- Witman, G. B., Plummer, J. and Sander, G.** (1978). *Chlamydomonas* flagellar mutants lacking radial spokes and central tubules. Structure, composition, and function of specific axonemal components. *J. Cell Biol.* **76**, 729-747.
- Yagi, T. and Kamiya, R.** (2000). Vigorous beating of *Chlamydomonas* axonemes lacking central pair/radial spoke structures in the presence of salts and organic compounds. *Cell Motil. Cytoskeleton* **46**, 190-199.
- Yang, P., Deiner, D. R., Rosenbaum, J. L. and Sale, W. S.** (2001). Localization of calmodulin and dynein light chain LC8 in flagellar radial spokes. *J. Cell Biol.* **153**, 1315-1326.
- Zhang, H. and Mitchell, D. R.** (2004). Cpc1, a *Chlamydomonas* central pair protein with an adenylate kinase domain. *J. Cell Sci.* **117**, 4179-4188.
- Zhang, Z., Sapiro, R., Kapfhamer, D., Bucan, M., Bray, J., Chennathukuzhi, V., McNamara, P., Curtis, A., Zhang, M., Blanchette-Mackie, E. J. and Strauss, J. F., III** (2002). A sperm-associated WD repeat protein orthologous to *Chlamydomonas* PF20 associates with Spag6, the mammalian orthologue of *Chlamydomonas* PF16. *Mol. Cell Biol.* **22**, 7993-8004.
- Zhang, Z., Jones, B. H., Tang, W., Moss, S. B., Wei, Z., Ho, C., Pollack, M., Horowitz, E., Bennett, J., Baker, M. E. and Strauss J. F., III** (2005). Dissecting the axoneme interactome: The mammalian orthologue of *Chlamydomonas* PF6 interacts with SPAG6, the mammalian orthologue of *Chlamydomonas* PF16. *Mol. Cell Proteomics.* **4**, 914-23